

Linearization of Optical IMDD Transmission Systems Using Accelerated Iterative Algorithms

Shaohua Hu^(1,2), Jianming Tang⁽²⁾, Jing Zhang⁽¹⁾, Kun Qiu⁽¹⁾

⁽¹⁾ Key Laboratory of Optical Fibre Sensing and Communications (Education Ministry of China), University of Electronic Science and Technology of China, Chengdu, Sichuan 611731, China. zhangjing1983@uestc.edu.cn

⁽²⁾ School of Electronic Engineering, Bangor University, Bangor, LL57 1UT, UK.

Abstract We propose two algorithms accelerating DSP processes of linearizing IMDD systems. C-band 100 Gb/s PAM4 transmissions over 200 km SSMFs are demonstrated numerically without any modifications to installed physical layer systems. The algorithms significantly outperform conventional nonlinear equalization and iterative algorithms.

Introduction

For 5G-oriented optical access networks and data centre interconnections, intensity modulation and direct detection (IMDD) transmission systems are preferable due to their cost-effectiveness and low complexity. However, unlike coherent optical transmission systems, the fibre chromatic dispersion is difficult to be compensated after square-law detection^[1]. The square-law detection-induced signal-signal beating has been explored extensively. Kramers-Kronig (KK) receivers^[2], single sideband (SSB) technique^[3], delay interferometer (DI)^[4] and stokes vector receivers (SVR)^[5] are the typical examples of previously reported techniques that can reconstruct the optical field and then perform the signal recovery operation. They are effective for the system linearization however they require considerable modifications to physical layer IMDD transmission systems.

Recently, an iterative field retrieval algorithm originating from the G-S algorithm developed for optical imaging shows good potential for further improving the signal transmission capacity of the IMDD optical transmission systems. In the previously published work, the modified Gerchberg-Saxton (G-S) algorithms can be applied at the transmitter and the receiver for pre-emphasis and post-compensation, respectively^[6, 7]. These algorithms work well in field retrieval without pilot symbols. However, they suffer a local optimum problem where the error estimation does not improve after several iterations. To enhance their performance, pilot symbols are introduced in the algorithms. However it needs two photodiodes (PD), one dispersive device, and hundreds or thousands of iterations to approach an acceptable global optimum^[8]. In this paper, we demonstrate the effectiveness of periodically-inserted pilot symbols for IMDD systems without requiring any structure modifications. The technique is termed data-aided iterative algorithm (DIA), which is very

simpler than previously reported algorithms^[8]. Moreover, we show an acceleration strategy by introducing symbol hard-decisions to increase the number of pilot symbols, named decision-directed DIA (DD-DIA), which can support >100 Gb/s PAM4 optical signals over 200 km IMDD transmissions with <60 iterations. The proposed technique considerably outperforms conventional iterative algorithms in terms of minimizing the iteration number required for reaching the FEC limit, signal reconstruction performance and transmission capacity improvement. This indicates the potential of practically implementing the technology in IMDD transmission systems for medium-reach applications.

Linearization Algorithms.

• DIA

To process the signal sequence after an analog-to-digital converter (ADC) at the receiver, we resample the signal by 2 samples per symbol. Assuming the signal is perfectly frame-synchronized, the DIA can be applied following the procedures illustrated in Fig. 1. We first initialize the phase by

$$\varphi_{R_init}(n) = 2\pi n / L_{Sig}, \quad (1)$$

where n is the time index and L_{Sig} is the sequence length. Then the signal is back-propagated in the digital domain by

$$T_1(f) = R_1(f)H_{CD}^{-1}(f) = \mathbf{F}[\sqrt{I(t)}e^{j\varphi_R(t)}]e^{j\pi D \frac{\lambda^2}{c} L_f^2} \quad (2)$$

where $\varphi_R(t)$ is the phase signal of the optical field propagated through the fiber, $I(t)$ is the optical current after the PD. In the digital domain, an analogue frequency f can be replaced with a digital angular frequency $\omega = 2\pi f T_s$ where T_s is the sampling interval. $T_1(\omega)$ is match-filtered and down-sampled to the baud rate and is subject to the pilot-symbol insertion, as expressed in Eq. (3) where H_{SRRC} , H_{MF} , \mathbf{F} , \uparrow^N , \mathbf{G} , and \downarrow_M represent square-root raise cosine filtering, match filtering, discrete Fourier transform, $N \times$ up-

sampling, pilot symbol insertion operation and $M \times$ down-sampling.

$$T(n) = \left| \begin{array}{l} H_{SRRC}(n) \otimes \\ \left\{ \uparrow^2 \left\{ G \left\{ \mathbf{F}^{-1} \left\{ \downarrow_2 \left[T_1(\omega) H_{MF}(\omega) \right] \right\} \right\} \right\} \right\} \right| e^{j\varphi_{Chirp}(n)} \quad (3)$$

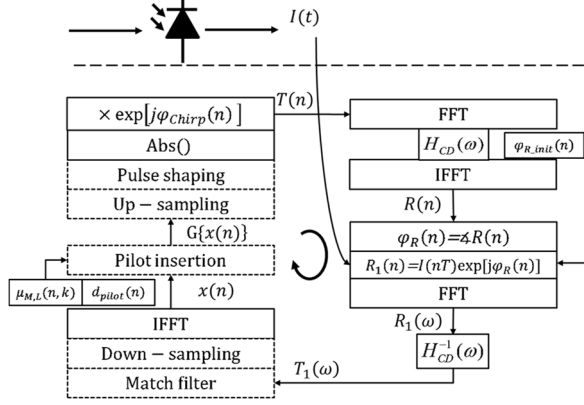


Fig.1: Data-aided iterative algorithm

The pilot symbol allocation strategy described in $G\{x(n)\}$ is expressed as

$$\begin{cases} G\{x(n)\} = \mu_{M,L}(n,k) d_{pilot}(n) + [1 - \mu_{M,L}(n,k)] x(n) \\ \mu_{M,L}(n,k) = \begin{cases} 1, & \text{for } \text{mod}(n, M) = 0 \ \& \ \text{mod}(k, L) = 0 \\ 0, & \text{otherwise} \end{cases} \end{cases} \quad (4)$$

where $\mu_{M,L}(n,k)$ is the flag representing whether we insert pilot symbols to $T_1(t)$ at a specific time and iteration slots. M , L , n , and k represent the time interval, the iteration interval, the time index and the iteration index respectively. Taking Fig. 2 as an example, the following parameters are taken: $M=8$, $L=3$ and an overhead of $1/M \times 100\% = 12.5\%$. The pilot insertion operation is only enabled at the 1-st, 4-th, 7-th cycles of iteration. For the rest of iterations, Eq. (4) is simplified to conventional iterative algorithm (IA), as shown below

$$T(n) = \left| \mathbf{F}^{-1} [T_1(\omega)] \right| e^{j\varphi_{Chirp}(n)}, \quad (5)$$

The pilot symbols further improve the convergence at neighboring symbols and iterations.

The newly constructed signal is forward-propagated through the fiber to obtain $R(n)$. The angle part of $R(n)$ is then abstracted, which is regarded as an estimated phase of the received optical field. Note that the intensity of the optical field is the detected discrete time signal after the ADC. The above describes the procedures associated with one iteration of the proposed DIA technique.

- DD-DIA

To enhance the linearization performance, we introduce hard-decision before the pilot insertion operation. The recovered symbols are randomly

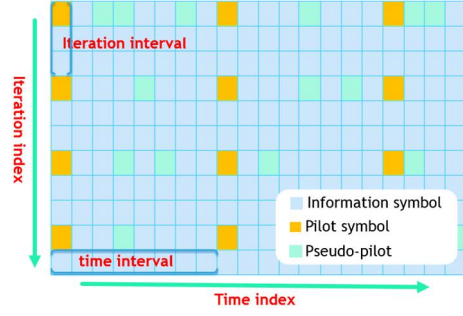


Fig. 2: Allocation of pilot and pseudo-pilot symbols

selected, which are then taken as additional pilot symbols, as shown in Fig. 2. As such symbols do not increase the overhead, we refer them to as pseudo-pilot symbols. To avoid large decision error-induced algorithm operation failure, use is made of the DIA for pre-convergence to guarantee its stability, this is termed decision-aided DIA (DD-DIA). DD-DIA provides an opportunity for DIA to have different pilots at different iterations, and accelerates the signal reconstruction regardless of the existence of incorrect pilot symbols.

Simulations and discussions.

To verify the performance improvement associated with the proposed DIA algorithm in IMDD optical transmission systems, we conduct numerical simulations using VPI 9.1, where a single carrier PAM4 signal is transmitted. Fig.3 shows the simulation setup of the considered PAM4 IMDD system.

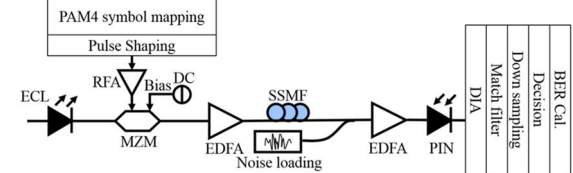


Fig. 3: Simulation diagram and DSP flowchart of the IMDD transmission system

At the transmitter, a PRBS data sequence is mapped into a PAM4 symbol sequence, which is then up-sampled by a factor of 2. The square-root raised cosine (SRRC) filter with a roll-off factor of 0.1 is applied to the up-sampled sequence to improve the spectral efficiency and partially illuminate CD-induced signal distortions. The electrical-to-optical (E/O) conversion is realized by a Mach-Zander modulator (MZM) biased at $V_{\pi}/4 = 2.5$ V, where the input continuous optical waveform operates at a wavelength of 1550.00 nm and has a linewidth of 100 kHz. The driving voltage amplitude of the RF input to the MZM is 0.4 V. To compare the performance between DIA, conventional IA, and the first 3 order Volterra nonlinear equalization, the baud rate is set to be 50 GBaud, and hence the output optical signal

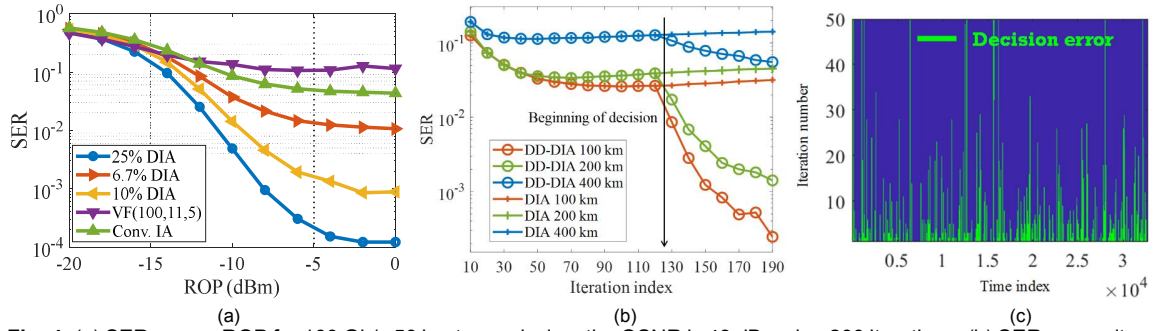


Fig. 4: (a) SER versus ROP for 100 Gb/s 50 km transmission, the OSNR is 43 dB, using 200 iterations; (b) SER versus iteration number for 100Gb/s PAM4. OSNR=40 dB, ROP=-4 dBm. (c) Decision error map for specific time and iteration slots..

from the MZM has a 50 GHz bandwidth and a 100 Gb/s data rate. An ideal power-controlled EDFA is deployed after the MZM to ensure that the launch power is fixed at -2 dBm. The fiber length is 50 km with a dispersion parameter of 16 ps/nm/km, which is identical to the G. 652 fiber. An optical AWGN source loads noise to the optical signal transmitted through the fiber in order to adjust optical signal's OSNR from 37 to 52 dB. The noise is calculated within a spectral resolution of 0.1 nm. At the receiver, to control the received optical power, a pre-amplifier is employed before the PIN photodiode where thermal noise and shot noise is considered. After optical-to-electrical (O/E) conversion in the receiver, the electrical current is sampled at 100 GSymbol/s. The receiver side DSP includes (DD-)DIA, match filtering, down sampling, and maximum likelihood symbol decision.

We compare the signal recovery performance for 100 Gb/s PAM4 over 50 km SSMF transmission in Fig. 4(a). It can be found that the conventional IA without pilot outperforms Volterra filter (VF) where the number of taps for the first three orders are 100, 11, and 5. Compared with the conventional IA, DIA with a 6.7% overhead of pilot symbols can reduce the SER below the 20% FEC limit. When the overhead increases from 6.7% to 10%, more than 3 dB received optical power (ROP) improvements can be obtained. We also find the number of pilot symbols significantly influences the SER performance. This is because the pilot data corrects the convergence orientation of the conventional iterative algorithm.

Consequently, we add the decision process after 120 cycles of DIA, i.e., DD-DIA, for signal reconstruction and sketch the convergence curves for various fiber lengths in Fig. 4(b). For each DD iteration, 60% recovered symbols are randomly selected as the pseudo-pilot symbols. One and two orders of magnitude SER reduction can be observed for 100 km and 200 km transmissions. The decision process yields the SER improvement even when the SER is 0.1, this

indicates the significantly improved robustness of the DD-DIA to the decision errors.

Finally, as mentioned in section 2, minor decision errors are not a dominant factor for the failure of the DD-DIA. To verify the statement, we depict decision errors at different iterations and time slots after enabling the DD-DIA in Fig. 4(c), where the narrow block in green represents the occurrence of decision errors. The OSNR, ROP, fiber length and bitrate are set to be 43 dB, -4dBm, 200km and 100 Gb/s, respectively. In the decision error map, the 2-D plane is gridded up by the iteration number and time index, where we can figure out the error occurrence along the iteration number for the n -th symbol. We find most decision errors rapidly disappear and are less likely to reoccur once it is corrected. When the DD process lasts about 30 cycles, most of the errors are corrected by the combination of decision and DIA, which is consistent with Fig. 4(b). Therefore, The DD-DIA can significantly accelerate the convergence speed compared to the DIA without increasing the overhead of pilot symbols.

Conclusions

We have proposed two novel acceleration algorithms including DIA and DD-DIA to linearization IMDD systems. The algorithms improve the convergence and signal reconstruction performances, and can support >100 Gb/s PAM4 over 200 km optical fibre transmissions.

Acknowledgements

This work was supported in part by the DESTINI project funded by the ERDF under the SMARTExpertise scheme, the DSP Centre funded by the ERDF through the Welsh Government, in part by the NSFC (61871082 and 61420106011), the state Key Laboratory of Advanced Optical Communication Systems and Networks, Shanghai Jiao Tong University (2020GZKF014), Fundamental Research Funds for the Central Universities (ZYGX2019J008) and China Scholarships Council (No. 201906070011).

References

- [1] C. Sun, D. Che, H. Ji, and W. Shieh, "Study of Chromatic Dispersion Impacts on Kramers–Kronig and SSBI Iterative Cancellation Receiver," *IEEE Photon. Technol. Lett.*, vol. 31, no. 4, pp. 303-306, 2019.
- [2] A. Mecozzi, C. Antonelli, and M. Shtaif, "Kramers–Kronig coherent receiver," *Optica*, vol. 3, no. 11, pp. 1220-1227, 2016.
- [3] X. Ruan, L. Zhang, F. Yang, Y. Zhu, Y. Li, and F. Zhang, "Beyond 100G Single Sideband PAM-4 Transmission With Silicon Dual-Drive MZM," *IEEE Photon. Technol. Lett.*, vol. 31, no. 7, pp. 509-512, 2019.
- [4] X. Li *et al.*, "Transmission of 4×28-Gb/s PAM-4 over 160-km single mode fiber using 10G-class DML and photodiode," in *2016 Optical Fiber Communications Conference and Exhibition (OFC)*, 2016, pp. 1-3.
- [5] D. Che, C. Sun, and W. Shieh, "Maximizing the spectral efficiency of Stokes vector receiver with optical field recovery," *Opt. Express*, vol. 26, no. 22, pp. 28976-28981, 2018.
- [6] G. Goeger, "Applications of Phase Retrieval in High Bit-Rate Direct-Detection Systems," in *2016 Optical Fiber Communication Conference (OFC)*, p. Th2A.40.
- [7] G. Goeger, C. Prodaniuc, Y. Ye, and Q. Zhang, "Transmission of intensity modulation-direct detection signals far beyond the dispersion limit enabled by phase-retrieval," in *2015 European Conference on Optical Communication (ECOC)*, 2015, pp. 1-3.
- [8] H. Chen, N. K. Fontaine, J. M. Gene, R. Ryf, D. T. Neilson, and G. Raybon, "Dual Polarization Full-Field Signal Waveform Reconstruction Using Intensity Only Measurements for Coherent Communications," *J. Lightwave Technol.*, vol. 38, no. 9, pp. 2587-2597, 2020.